Ancione Giuseppa

Milazzo Maria Francesca
University of Messina, Messina, Italy

Salzano Ernesto
Instituto di Ricerche sulla Combustione, Consiglio Nazionale delle Ricerche, Napoli, Italy

Maschio Giuseppe
University of Padova, Padova, Italy

Semi-automatic geo-processing procedure for the vulnerability mapping of industrial facilities in areas with the potential volcanic ash fallout

Keywords

Na-Tech risk, vulnerability mapping, threshold value, ash fallout; exceedance probability, geoprocessing

Abstract

Following recent severe natural events, attention has been focused on industrial installations located in areas prone to natural hazards. This work concerns the study of volcanic Na-Tech events (i.e. technological risks triggered by natural causes) and aims at defining a procedure for the representation of the vulnerability of industrial facilities in areas with the potential volcanic ash fallout by means a Geographical Information System (GIS). Here, we focused on the construction of a semi-automatic procedure for the vulnerability mapping for cases where input data is very limited; it is based on the use of a specific tool named ModelBuilder of the ArcGIS software.

1. Introduction

In the framework of the Quantitative Risk Analysis for chemical facilities, the vulnerability may be defined as the probability of occurrence of a certain damage (e.g. probability of injury), given the occurrence of an incidental scenario due to the release of hazardous materials.
In the framework of natural hazards, the vulnerability of a system to a potential incidental scenario is usually described by combining the susceptibility (inherent propensity to damage) and the resilience (propensity to deal with the emergency and the recovery of normal activity) of the territory [17]. The vulnerability is a function of the distance with respect to the source of the event. Vulnerability maps can be drawn when the correlation between the vulnerability and the distance is known. These are useful to manage natural and industrial risks, but also for emerging risks, such as technological risks triggered by natural causes (Na-Tech events). As reported by [15], over the years, an increase of Na-Tech events has been observed due to different causes, such as the expansion of the industrialization and urbanization in the territory, climate changes, etc. Such elements increased the awareness about Na-Tech events and concurred to consider these scenarios as emerging risks.
Past catastrophic events highlighted the high destructive potential of Na-Tech scenarios, but only during these last years, researchers have focused their attention on this issue. As a matter of the fact, the analysis of recent literature has shown that many countries have to face natural hazards, but none appears to have an appropriate management plan based on the definition of Na-Tech vulnerability maps [4]. These considerations suggest that improving the knowledge of the vulnerability of industrial facilities to Na-Tech events and developing vulnerability maps as tools for decision making is actually necessary [8].

This paper is focused on the implementation on a Geographical Information System (GIS) of the procedure developed by [8] for the vulnerability assessment of industrial facilities. The easier management of geographical data (georeferenced) and other related information, through a GIS software, allows to calculate the vulnerability associated with each point of the territory and, then, the cartographical representation. The use of a GIS, in this case, also allowed the development of semi-automatic procedures for the vulnerability mapping.
In section 2 the implementation of the semi-automatic procedure is described. A case-study, related to the area surrounding the volcano Etna (Italy) and describing the application of the whole methodology, is given in the third part of the paper.

2. Methodology for vulnerability mapping

The methodology described in this section is a generic and simplified approach for estimating the vulnerability of industrial facilities to volcanic Na-Tech events. As mentioned above, it has recently been proposed by [8]. The whole approach is summarized in the flow-chart of *Figure 1*.

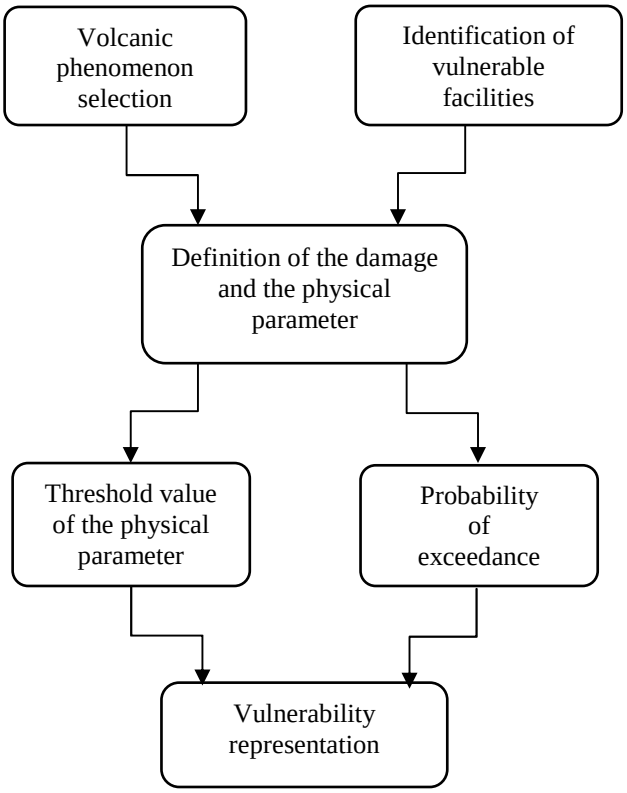

Figure 1. Flow-chart for the representation of vulnerability

The first step concerns the choice of a specific volcanic phenomenon (characterised by a given occurrence and magnitude) and the selection of a vulnerable facility located in the surrounding of the volcano. Hence, it is necessary to define a potential damage with respect to the physical parameter, associated with the magnitude of the selected volcanic phenomenon, which causes the failure of the facility. Then, a threshold value of the parameter and the probability of exceeding this limit must be estimated. Finally, by using both these estimates, the vulnerability mapping is possible.
In order to apply the procedure of *Figure 1*, a general knowledge of the territory is necessary, as well as a careful collection of meteorological statistics and historical information about the volcanic eruptions. This information is important to derive a number of simulation maps from which the exceedance probability curves of physical parameters are derived.
This contribution focuses on the last step of the method of *Figure 1*. Quite clearly, in order to achieve the vulnerability mapping, it is necessary to estimate the probabilities also for the points where these are not known. This operation can be made through a spatial interpolation method. To this regard, it is worth mentioning that there are several interpolation procedures, each of them characterized by a different time for the data elaboration, accuracy, sensitivity to parameters variation and degree of smoothness of the interpolated surface. These procedures can be grouped in two main classes: deterministic and stochastic methods [6]. Deterministic approaches are based on a correlation among neighbouring points whose parameters have an explicit physical meaning; stochastic methods correlate neighbouring points through a statistical relation. The class of deterministic procedures includes geometric methods (area interpolation method), Inverse Distance Weighting (IDW) method (named also Point Interpolation Method); finally the class of stochastic methods procedures includes the Kriging and Cokriging methods [6].
The spatial interpolation assumes that the data is a continuous spatial function [16]. Waters [18] states that using data related to a series of points, as in our case, the choice of interpolation method is crucial because it approximates a representation in the space of the physical phenomenon (in this case volcanic ash fallout). Both the quality of the original data and the interpolation method are essential to give a reliable estimate. Some causes of a non-optimal estimate are:

a) few available points;
b) limited spatial coverage of the points;
c) uncertainty about the location and the value of the measured physical quantity.

In the following each step of the procedure is described using a case-study.

3. An example of application

An application to the area surrounding Mt. Etna shows how the results of previous studies related to the analysis of the effects of ash fallout on chemical facilities [10], [11], can be processed to achieve a semi-automatic vulnerability mapping (final step of the procedure of *Figure 1*).

3.1. Volcanic phenomenon

Mt. Etna is one of the most active volcano in Europe, it is located in Sicily (Italy) and has recently changed its eruptive style giving more frequent explosive eruptions with ash emissions. The territory surrounding the volcano is characterised by the presence of the city of Catania with more than 300 thousand inhabitants, by many small urban centres and agricultural and industrial areas. Mt. Etna is characterized by an explosive activity having a VEI (Volcanic Explosive Index [13]) equal to 2 or 3. Among the numerous volcanic phenomena (lava flows, pyroclastic flows, lahars), which can potentially damage population and structures, the volcanic ash (named also tephra) fallout seems the most significant phenomenon, this is due mainly to both its large impact area and the location of the industrial sites. Local weather conditions significantly influence the distance of ash fallout [9], in some case, the tephra reached also the site southern site of Priolo-Augusta.
The potential damages, due to ash fallout on atmospheric storage tanks, either with fixed or floating roof, have been identified by [9]. They also developed models correlating the damage with respect to the ash load (physical parameter). The local vulnerabilities, related to both the most frequent and the worst explosive eruptions, were estimated by the same authors in [10].

3.2. Potential damage to storage tanks

To achieve our aim, we have focused on atmospheric storage tanks, but obviously the methodology proposed can be easily applied to other facilities. As given in [1], atmospheric storage tanks are typically classified as fixed roof tanks or floating roof tanks. Fixed roof tanks can be used for products, such as crude oil, gasoline, fuel oil, water, etc. Floating roof tanks are used to minimize product loss by evaporation of liquid fuels and, thus, to increase safety by minimizing the amount of vapour in the space between the roof and liquid.
The ash deposit load may be the cause of different failures, each of them is identified with a specific symbol *Tn* in the following list:

- Light damage to the structure of the fixed roof (T1);
- Severe structural damage to the structure of fixed roof (T2);
- Structural collapse of the fixed roof tank (T3);
- Sinking of the floating roof (T4);
- Capsizing of the floating roof tanks (T5).

3.3. Threshold values of volcanic ash load

The threshold limits of volcanic ash load, used to determine the probability of damage of atmospheric tanks with a fixed roof, were calculated by [14]. Milazzo derived the values for atmospheric floating roof tanks [9]. *Table 1* and *Table 2*, respectively, give the threshold values of the tephra load (kg/m^2) for fixed roof and floating roof tanks.

Table 1. Threshold values for volcanic ash load for the structural damage of fixed roof tanks

Damage	Light	Structural	Collapse
Symbol	T1	T2	T3
Ash load (kg/m^2)	122	357	714

Table 2. Threshold values for volcanic ash load for the structural damage of floating roof tanks

Damage	Sinking	Capsizing
Symbol	T4	T5
Ash load (kg/m^2)	680	380*

*With an asymmetrical ash distribution causing the immersion of half roof [9].

3.4. Probability of exceedance of the physical parameter

The vulnerability (or fragility) of the equipment is known when the probability of exceedance of the physical parameter and its threshold value are also known.
Concerning the case-study, Barsotti et al. have produced exceedance probability curves for tephra deposit, at the ground level and related to the most frequent and the worst explosive scenarios of Mt. Etna [3]. An example of exceedance curve is given in *Figure 2*. Each curve is obtained through several numerical simulations of the explosive phenomenon. However, as expected, these simulations are complex and time-consuming, for this reason current literature provides only few studies of this type. Even Barsotti

et al. derived exceedance probability curves only for few locations surrounding Mt. Etna.

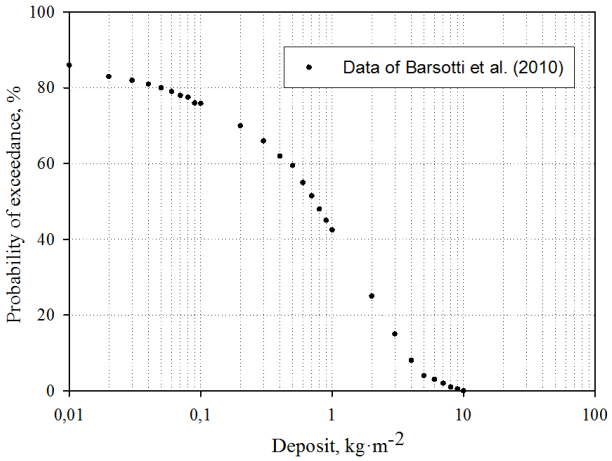

Figure 2. Example of an exceedance probability curve of ash ground deposit as produced by Barsotti et al

3.5. Vulnerability mapping

The main difficulty in elaborating vulnerability maps for facilities in area prone to ash fallouts, is that input data is very limited. As evidenced in the previous section, probabilities are usually known only for few locations. By means of a spatial interpolation method it is also necessary to estimate the probabilities for the points where these are not known.
The input data to map the vulnerability for the case-study are given in *Figure 3*. The map shows the spatial distribution of the locations investigated. In this figure, the vulnerability of the atmospheric storage tanks to the ash fallout with respect to a specific damage (in this case the light damage T1) is represented using circles. The area of each circle is proportional to the value of the probability of exceedance of the threshold value T1.
In this study we have applied two spatial interpolation methods, these are the IDW and the Kriging methods. In Section 4, the results of the application of both procedures and the comparison between them are shown.

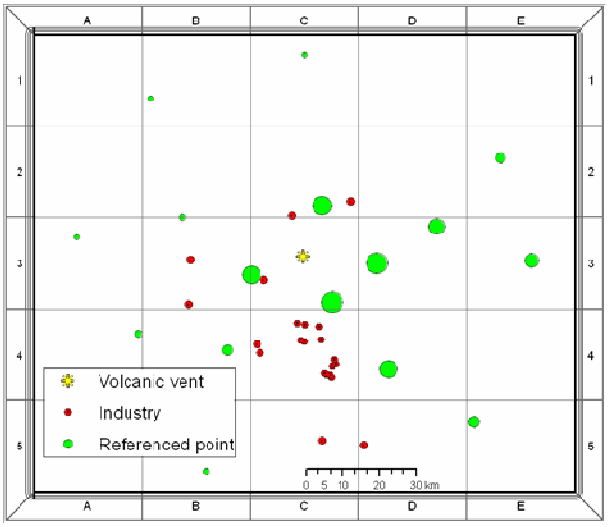

Figure 3. Spatial distribution of points and exceedance probabilities for T1

The IDW method (determinist) assumes that each measurement has a local influence, which decreases with the distance. It is based on the following mathematical function:

$$z_{(So)} = \frac{\sum_{i=1}^{N} w_i \cdot z_{(Si)}}{\sum_{i=1}^{N} w_i} \qquad (1)$$

where: $z_{(So)}$ is the value to be predicted associated with the location S_o (prediction point); N is the number of locations used for the estimation (identification number for the points around the prediction point); i = 1, 2, 3, ...; $z_{(Si)}$ is the measured value of the variable at the i-th location; $w_i=1/d_i^2$ is the weight coefficient of the measured point at the i-th location and d_i is the distance between the i-th point and S_o.
The Kriging method (stochastic) is a geo-statistical procedure for data interpolation [2], [5]-[6]. The interpolation model takes into account the value of the variable in the other locations and a weight coefficient based not only on the distance between the measured points (as the IDW approach), but also on the overall spatial arrangement of the measured points. This means that it is based on a probabilistic elaboration in order to develop more complex predictive models. The correlation for the interpolation is given by following equation (2):

$$z_{(So)} = \sum_{i=1}^{N} \lambda_i \cdot z_{(Si)} \qquad (2)$$

where: λ_i is the weight assigned to each measured point at the i-th location, it is based not only on the

distance between the measured points and the prediction location but also on the overall spatial arrangement of the measured points.
The use of the Kriging allows including the estimation of the error and the uncertainty associated with each prediction [6].

3.6. Semi-automatic geoprocessing

In this paper we focused on the construction of a semi-automatic method for vulnerability maps using a Geographic Information System software (the acronym GIS is often used).
A GIS is a system designed to capture, store, manipulate, analyze, manage, and present all types of geographical data. In the simplest terms, for the purpose of this work, a GIS is the merging of cartography, statistical analysis and computer science technology. The *geoprocessing* is a basic function of a GIS for the processing of geographical data. A typical *geoprocessing* operation takes an input dataset, performs an operation on that dataset and returns the result of the operation as an output dataset. It allows creating new information through the application of many operations to the existing data. An example, where *geoprocessing* has been applied to manage emergency originated by terrorist actions, is given in [12].
To achieve our aim, we used the GIS software developed by Esri, named ArcGIS, and performed our elaborations by means of a specific tool of the software, named ModelBuilder. This tool permits to create and manage sequences of *geoprocessing*. It feeds the outputs of an operation into another one, thus these outputs become the inputs to the following operation.
We created a simple model to elaborate the vulnerability of atmospheric storage tanks to volcanic ash deposits. It allows a quick vulnerability mapping and is based on the use of both the interpolation procedures described above. *Figure 4* shows the flow-chart of the whole procedure.
The model runs in a semi-automatic mode, thus, the *geoprocessing* operations could also be executed by users that do not have knowledge about GIS. Users will only have to collect the following input data:

- territorial sample points,
- probabilities of exceedance of ash load (probabilities of exceedance curves),
- the *Z* value field (*Figure 5*), that is the probability of exceedance of the threshold value of the ash load, which is the data that the user wants to interpolate.

Finally the *geoprocessing* model provides the map related to the interpolation method chosen.

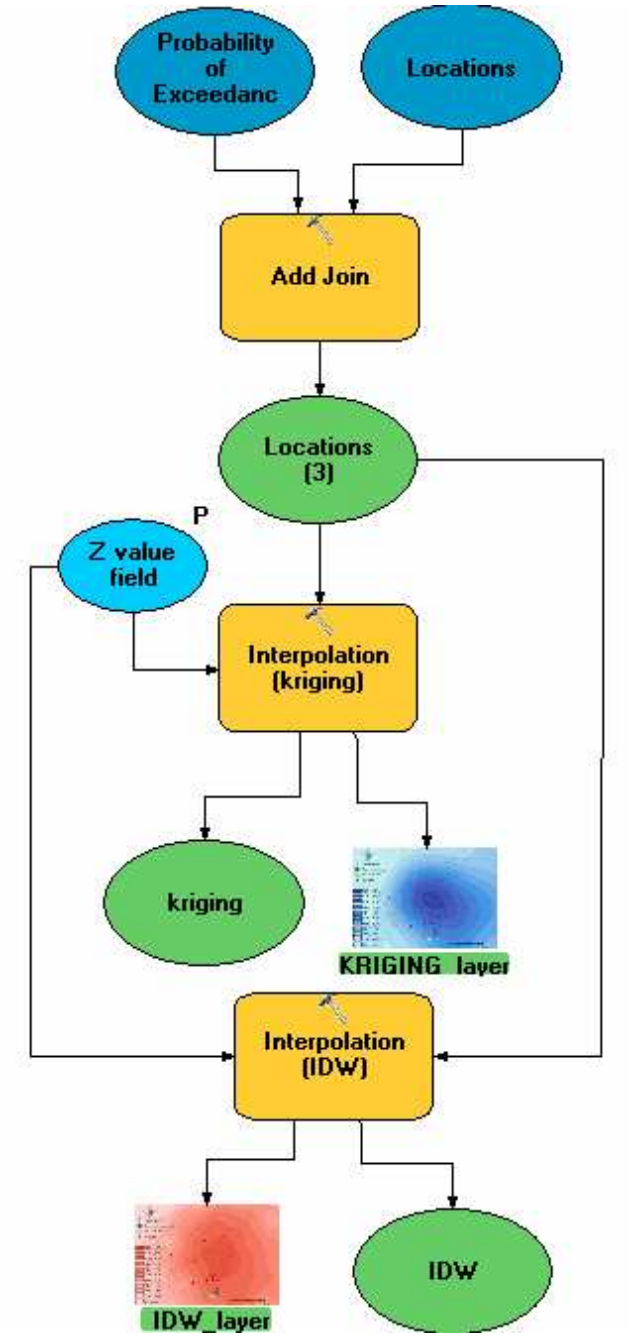

Figure 4. Flow-chart for the semi-automatic vulnerability mapping.

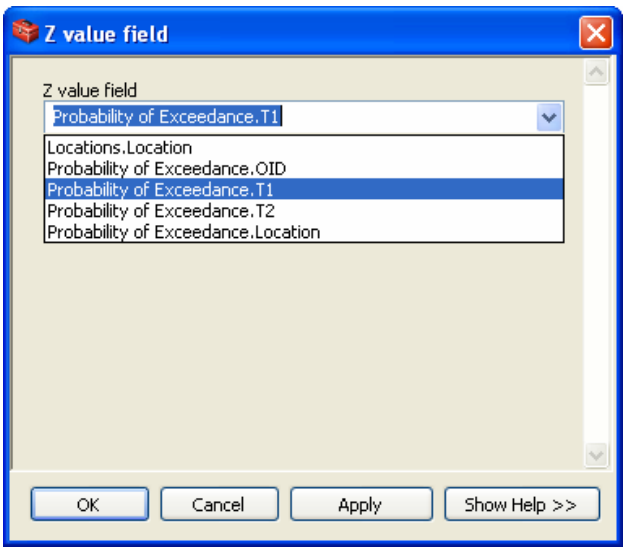

Figures 5. Selection of the probability of exceedance of a specific ash load

4. Results

Vulnerability maps for the case-study, related to the light damage of fixed roof storage tanks, are shown in *Figure 6* and *Figure 7*, using iso-probability curves on the cartography. These maps have been made using both the interpolation methods, described in the previous section.

A legend of colours has been defined; each colour is associated with a class of exceedance probabilities and the darkest colours represent an increase of the vulnerability.

Some considerations can be made related to the application of these interpolation methods. The IDW technique allows a quick calculation, but results are not very accurate. The geostatistical approach (Kriging method) requires a greater number of information for an accurate estimation and the data-processing is time-consuming, but it provides more details. The Kriging attenuates the local variability of the variable, it provides estimates that may exceed the minimum and/or maximum of the measured values, whereas the deterministic methods produce estimates within the range of values sampled [7].

It is important to validate each prediction. The validation procedure used in this work is named *cross-validation*, it consists in plotting the predicted value as a function of the measured value in a Cartesian graph. The data fitting gives a line, whose slope allows to comment about the applicability of the interpolation method. The model is applicable if the slope of the line is about 1.

Results of the validation procedure are shown in *Figure 8(a)* and *Figure 8(b)*.

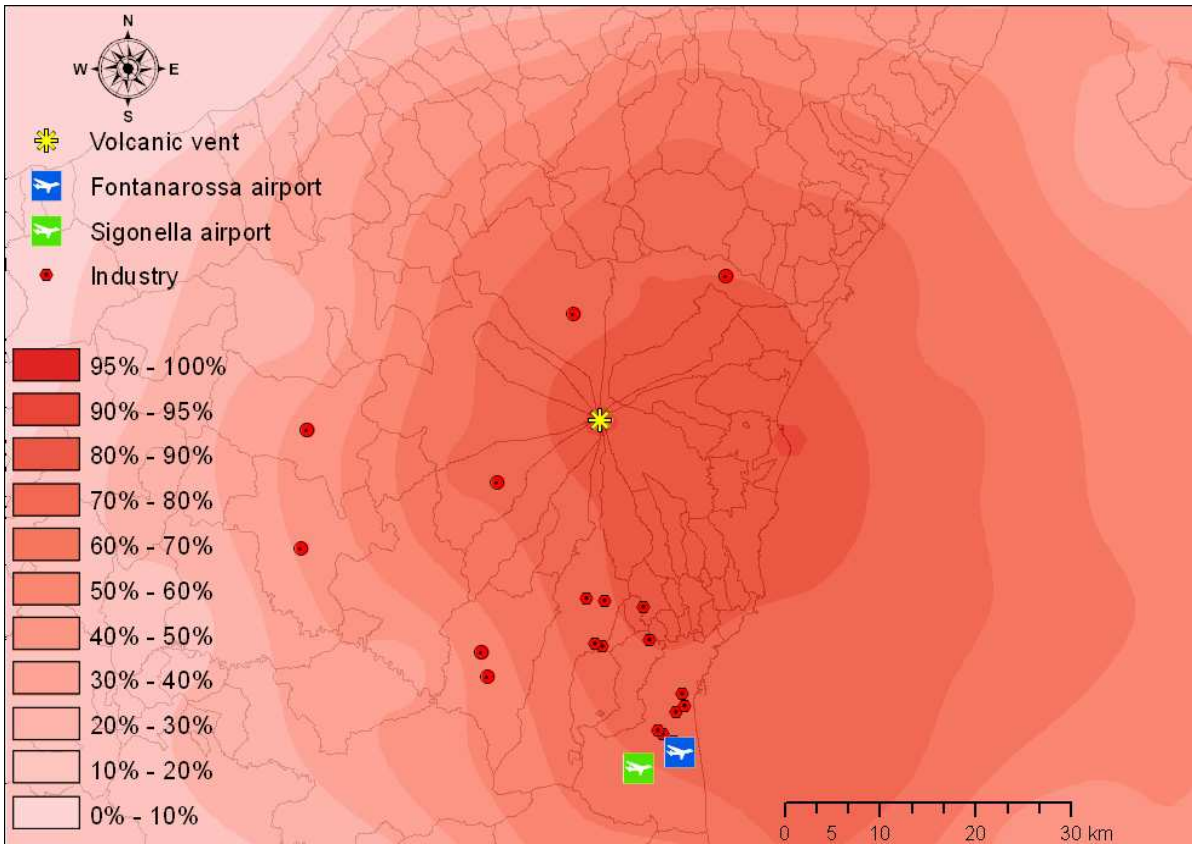

Figure 6. Vulnerability map for light damage (T1) to fixed roof storage tanks using the deterministic approach of Inverse Distance Weighting

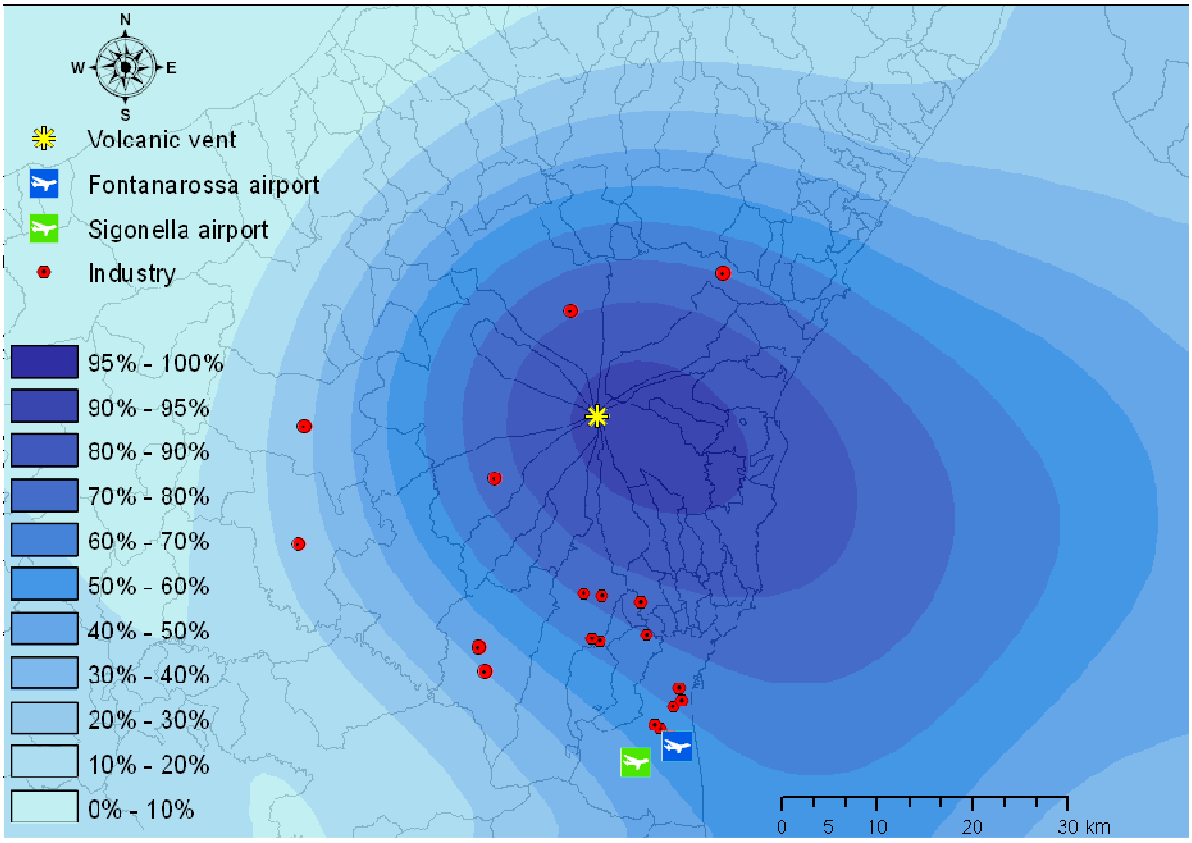

Figure 7. Vulnerability map for light damage of fixed roof storage tanks (T1) using the geostatistical approach of Kriging.

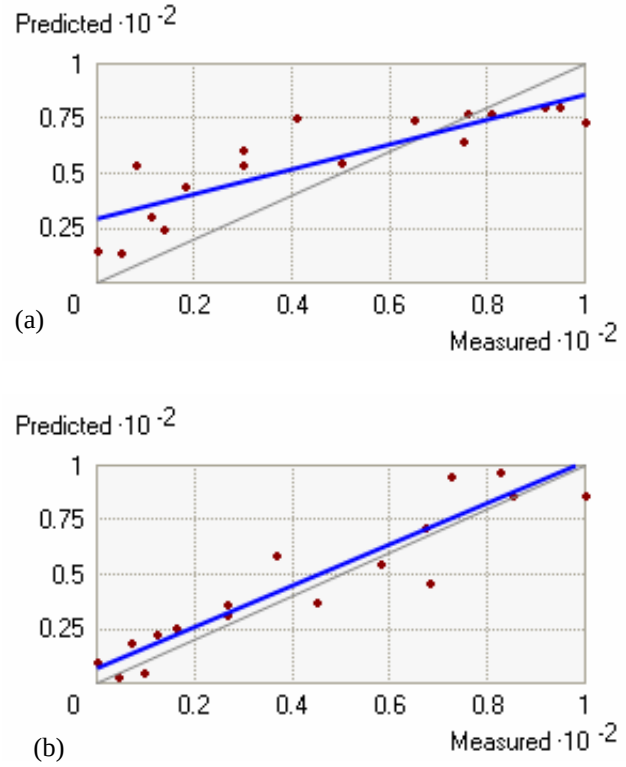

Figures 8. Validation of the prediction using (a) IDW method and (b) Kriging method.

The prediction of *Figure 8(b)* gives a slope close to 1 and demonstrates a good applicability of the Kriging method.

As described above, the semi-automatic procedure is very user-friendly. It allows a quick vulnerability mapping by means of different methods of interpolation. The execution is fast and can be made also by users with a limited knowledge about GIS.

6. Conclusions

A procedure for the estimation of the vulnerability and the construction of relative maps has been improved. The main aim was to provide local authorities and planners useful tools for the planning of emergencies connected to volcanic Na-Tech risks.

The method proposed in this work is applicable to any case study and is also useful when the exceedance probability is known for a limited number of points, in this case the choice of the interpolation model is the critical step of the whole procedure.

The ArcGIS software of Esri has been used to implement a semi-automatic procedure for vulnerability mapping by means of the ModelBuilder tool, which allows the automatic execution of various queries related to the analysis, the creation and display of maps. The procedure is characterized by a

fast execution. Several advantages result from the development of such a procedure including, for example, the saving of time during the emergency and the simplification of the work of risk managers.

Acknowledgements

This research has been supported by the MIUR funded project PRIN 2008 entitled "Analysis of potentially critical scenarios on industrial installations and the infrastructure of Eastern Sicily and of health risks associated with explosive eruptions of Etna".

References

[1] American Petroleum Institute API. (1988) *Welded steel tanks for oil storage.* Document API 650, USA.

[2] Bailey, T.C. & Gatrell, A.C. (1995). *Interactive spatial data analysis*. Addison Wesley Longman Ltd, Harlow.

[3] Barsotti, S., Andronico, D., Neri, A., Del Carlo, P., Baxter, P.J., Aspinall, W.P. & Hincks, T. (2010). Quantitative assessment of volcanic ash hazards for health and infrastructure at Mt. Etna (Italy) by numerical simulation. *J. Volcanol. Geoth. Res.*, 192, 85–96.

[4] Cruz, A., Steinberg, L.J., Vetere Arellano, A. L., Nordvik, J. P. & Pisano, F. (2004). *State of the Art in Natech Risk Management: NATECH: Natural Hazard Triggering a Technological Disaster.* ISDR International Strategy for disaster Reduction. EUR 21292 EN, Ispra. (Report).

[5] Hengl, T., Heuvelink, G.B.M. & Stein, A. (2004). A generic framework for spatial prediction of soil variables based on regression-kriging. *Geoderma*. 120, 75-93.

[6] Johnston, K., Ver Hoef, J.M., Krivoruchko, K. & Lucas, N. (2004). *Arcgis9: Using ArcGis Geostatistical Analyst*. Esri. Redlands.

[7] Liebhold, A.M., Rossi, R.E. & Kemp, W.P. (1993). Geostatistics and Geographic Information Systems in applied insect ecology. *Annu. Rev. Entomol.* 38, 303-327.

[8] Milazzo, M.F., Lisi, R., Ancione, G., Lister, D.G. & Maschio, G. (2012). Vulnerability maps for industrial facilities in areas with the potential volcanic ash fallout. *Proc. 11th International Probabilistic Safety Assessment and Management Conference and the Annual European Safety and Reliability Conference 2012, PSAM11 ESREL 2012*. 7, 5388-5397.

[9] Milazzo, M.F., Ancione, G., Lister, D.G., Salzano, E., Basco, A. & Maschio, G. (2012). Analysis of the effects due to fallout of ash from Mt. Etna on industrial installations. *Chem. Eng. Trans,*. 26, 123-128.

[10] Milazzo, M.F., Ancione, G., Basco, A., Lister, D.G., Salzano, E. & Maschio, G. (2013). Potential loading damage to industrial storage tanks due to volcanic ash fallout. *Nat. Hazards*, 66 (2), 939-953.

[11] Milazzo, M.F., Ancione, G., Salzano, E., Lister, D.G. & Maschio, G. (2012). Potential damage to filtration systems due to volcanic ash fallout. *Proc. 11th International Probabilistic Safety Assessment and Management Conference and the Annual European Safety and Reliability Conference 2012, PSAM11 ESREL 2012*. 7, 5379-5387.

[12] Milazzo, M.F., Ancione, G., Lisi, R., Vianello, C. & Maschio, G. (2009). Risk management of terrorist attacks in the transport of hazardous materials using dynamic geoevents. *J. Loss Prevent. Proc.* 22 (5), 625-633.

[13] Newhall, C.G. & Self, S. (1982).The Volcanic Explosivity Index (VEI): an estimate of the explosive magnitude for historical volcanism. *J. Geophys. Res*. 87, 1231–1238.

[14] Salzano, E. & Basco, A. (2008). A preliminary analysis of volcanic Na-Tech risks in the Vesuvius area. *Proc. of the ESREL 2008*, 4, 3085-3092.

[15] Showalter, P.S. & Myers, M.F. (1994). Natural Disasters in the United States as Release Agents of Oil, Chemicals, or Radiological Materials Between 1980-9: Analysis and Recommendations. *Risk Analysis*, 14, 2, 169-181.

[16] Tobler, W. (1970). A computer movie simulating urban growth in the Detroit region. *Econ. Geogr*. 46(2), 234-240.

[17] United Nations Disaster Relief Coordinator UNDRO. (1982). *Natural Disasters and Vulnerability Analysis*. Report of Expert Group Meeting on Vulnerability Analysis, Geneva.

[18] Waters N.M. (1988). *Expert Systems and Systems of Experts, in Geographical Systems and Systems of Geography: Essays in Honour of William Warntz*. Coffey W.J., London (Ontario).